First-principles theory of magnetocrystalline anisotropy of disordered alloys: Application to cobalt platinum

S. S. A. Razee and J. B. Staunton
Department of Physics, University of Warwick, Coventry CV4 7AL, United Kingdom

F. J. Pinski
Department of Physics, University of Cincinnati, Ohio 45221

(Received 16 April 1997)

We present a first-principles theory of magnetocrystalline anisotropy of disordered alloys within the framework of the spin-polarized fully relativistic Korringa-Kohn-Rostoker coherent-potential approximation in which relativistic effects such as spin-orbit coupling and magnetization are treated on an equal footing. Unlike in some other methods, we calculate the magnetocrystalline anisotropy energy (MAE) of a material directly rather than subtracting the total energies of the material for two magnetization directions calculated separately. Since the total energy of a system is several orders of magnitude larger than its MAE ($\sim \mu$ eV), this approach provides a robust method. Our predictions of the MAE and magnetic easy axis of elemental bcc-Fe, fcc-Co, and fcc-Ni are in reasonable accord with previous calculations as well as with the experimental results. We calculate the MAE of disordered fcc-Co_xPt_{1-x} alloys for $x=0.25$, 0.5, and 0.75 and find that the magnetic easy axis for these alloys is along the [111] direction of the crystal, and that the magnitude of MAE is largest for the equiatomic composition. We also find that the magnitude of MAE decreases with temperature in these alloys, but the magnetic easy axis remains unchanged. [S0163-1829(97)02538-1]

I. INTRODUCTION

In recent years, the magnetocrystalline anisotropy of ferromagnetic materials containing transition metals has received attention, both theoretically and experimentally, because of the technological implications in high-density magneto-optical storage media.[1–3] To make these materials useful for future magneto-optical recording systems, a detailed understanding of the mechanism of this anisotropy is needed. Several experimental studies have been devoted to understand its origin and also to correlate it with other physical properties of the materials.[4–13] However, an *ab initio* theoretical approach that can explain the underlying physics is most desirable, because it will help to predict new materials with such desired properties. Over the past few years, considerable progress has been made in this direction,[14–31] but a comprehensive explanation at the microscopic level is still lacking.

In a solid, the equilibrium direction of the magnetization is along one of the cystallographic directions. The energy required to alter the magnetization direction is called the magnetocrystalline anisotropy energy (MAE). Brooks[32] suggested that the origin of this anisotropy is the interaction of magnetization with the crystal field, i.e., the spin-orbit coupling. Most of the present day theoretical investigations on magnetocrystalline anisotropy use standard band structure methods within the scalar-relativistic local spin-density functional theory and treat spin-orbit coupling as a perturbation. The MAE is then calculated by using the force theorem,[33] which states that the difference in total energy of two states with similar charge density is given by the difference in the single-electron contributions to the total energy. In actual calculations, this is evaluated as the difference in the sum over all occupied single-electron energies. Several investigations have been reported within this approach for transition metals,[14,15] as well as for ordered transition-metal alloys[21,22] and layered materials[16–19] with varying degrees of success. Some controversy surrounds these perturbative approaches regarding the method of summing over all the ''occupied'' single-electron energies for the perturbed state which is not calculated self-consistently.[23–25] Freeman and co-workers[23] have argued that this ''blind Fermi filling'' is incorrect and proposed the state-tracking approach in which the occupied set of perturbed states are determined according to their projections back to the occupied set of unperturbed states. This approach, combined with the so-called torque method,[26] was used by these authors to calculate the MAE of multilayers.[27] More recently, Trygg *et al.*[28] included spin-orbit coupling self-consistently in the electronic structure calculations but within a scalar relativistic theory. They obtained good agreement with experiment for bcc-Fe, fcc-Co, and hcp-Co, but failed to obtain the correct magnetic easy axis for fcc-Ni.

We note that in almost all the above studies, the band structure methods used are not fully relativistic and thus these approaches might not be adequate for materials containing elements with f electrons. Moreover, Jansen[34] pointed out that, the spin-orbit coupling which is the origin of magnetocrystalline anisotropy, is essentially a relativistic phenomenon, and therefore, can be more appropriately described within a fully relativistic framework. Thus it is desirable to treat relativity and magnetization (spin polarization) on an equal footing. We also point out that, apart from this conceptual difficulty, in all of the previous investigations, either the total energy or the single-electron contribution to it (if using the force theorem) was calculated for two magnetization directions separately and MAE obtained by subtracting one from the other. However, the MAE which in many cases is of the order of μ eV, is several orders of

magnitude smaller than the total energy of the system. Therefore, it is numerically more precise to calculate the difference directly, rather than taking the above course.[35] Consequently, a fully relativistic theory of magnetocrystalline anisotropy is needed which, in addition, should facilitate the direct calculation of MAE. Strange *et al.*[36,37] have developed a relativistic spin-polarized version of the Korringa-Kohn-Rostoker (SPR-KKR) formalism to calculate the electronic structure of solids, and Ebert and co-workers[38] have extended this formalism to disordered alloys by incorporating coherent-potential approximation (SPR-KKR-CPA). This formalism has been successfully used to describe the electronic structure and other related properties of disordered alloys such as magnetic circular x-ray dichroism, hyperfine fields, magneto-optic Kerr effect, etc. by Ebert and co-workers.[39–45] Strange *et al.*[30] and more recently Staunton *et al.*[35] have formulated a theory to calculate the MAE of elemental solids within the SPR-KKR scheme, and this theory has been applied to Fe and Ni.[30,31] They have also shown that, in the nonrelativistic limit, MAE will be identically equal to zero, indicating that the origin of magnetic anisotropy is relativistic. In this paper we present a generalization of the theory of Staunton *et al.*[35] to disordered alloys.

Owing to the typically small magnitude of MAE ($\sim\mu$ eV) of transition metals and their alloys, we have first tested the accuracy of our method, and for this purpose, calculated the MAE of elemental bcc-Fe, fcc-Co, and fcc-Ni. As discussed below (in Sec. IV A), our method correctly predicts the easy axes of magnetization for all these elements, although the magnitude of MAE is somewhat smaller when compared to the experimental data.

We then use our method to calculate the MAE of disordered fcc-Co_xPt_{1-x} alloys. These alloys have attracted our interest because of the following reasons. Large magnetic anisotropy,[6,7] large magneto-optic Kerr effect signals compared to the Co/Pt multilayers in the whole range of wavelengths (820–400 nm)[8,9] make these alloys potential magneto-optical recording materials. The chemical stability of these alloys, a suitable Curie temperature, and the ease of manufacturing enhances their usefulness in commercial applications.[8] Furthermore, these alloys are important from the point of view of fundamental physics of magnetic anisotropy; in Co-Pt systems spin-polarization is induced by Co whereas spin-orbit coupling is stronger in Pt, and therefore, this is a good system to test our theory. We are not aware of any theoretical calculation of MAE of alloys which treats relativistic effects such as spin-orbit coupling and spin-polarization on an equal footing.

Most of the experimental work on Co-Pt alloys have been on the ordered tetragonal phase, which has a very large magnetic anisotropy ($\sim$400 μeV) and the magnetic easy axis is along the c axis.[6,7] We are not aware of any experimental work on the bulk disordered fcc phase of these alloys. However, some results have been reported for disordered fcc phase of these alloys in the form of thin films.[8–13] It is found that the magnitude of MAE is more than one order of magnitude smaller than that of the bulk ordered phase, and the magnetic easy axis varies with the film thickness. We believe that theoretical investigation on the bulk disordered alloys will also provide insight into the mechanism of magnetic anisotropy in the ordered phase as well as in thin films. In this paper, we investigate the magnetic anisotropy of the disordered fcc phase of Co_xPt_{1-x} alloys for $x=0.25$, 0.50, and 0.75. In our calculations, we have used the self-consistent potentials from spin-polarized scalar relativistic KKR-CPA calculations. Our calculations predict that the easy axis of magnetization is along the [111] direction of the crystal for all the three compositions, and the anisotropy is largest for $x=0.50$.

The paper is organized as follows. In Sec. II, we present the formulation. We start with a brief outline of the SPR-KKR-CPA method and then derive an expression for the MAE within this formalism. In Sec. III, we present the numerical details. Afterwards, we present our results in Sec. IV and in Sec. V, we draw some conclusions.

II. FORMULATION

Our theory of magnetocrystalline anisotropy is based on the relativistic spin-polarized density functional theory.[46–48] MacDonald and Vosko developed the theory for a many electron system in presence of a ''spin-only'' magnetic field, i.e., ignoring the diamagnetic effects. This is a suitable basis for describing electrons in condensed matter. Within this formalism, the relativistic Kohn-Sham-Dirac single particle equations, in presence of an external field, can be written as

$$\{-i\hbar c\,\boldsymbol{\alpha}\cdot\nabla+\boldsymbol{\beta}mc^2+\mathbf{I}V^{\mathrm{eff}}[n(\mathbf{r}),\mathbf{m}(\mathbf{r})] - \boldsymbol{\beta}\boldsymbol{\sigma}\cdot\mathbf{B}^{\mathrm{eff}}[n(\mathbf{r}),\mathbf{m}(\mathbf{r})]-\varepsilon_i\}\psi_i=0, \tag{2.1}$$

where

$$n(\mathbf{r})=\sum_i^{\mathrm{occ}}\mathrm{Tr}\psi_i^{\dagger}(\mathbf{r})\psi_i(\mathbf{r}), \tag{2.2}$$

$$\mathbf{m}(\mathbf{r})=\sum_i^{\mathrm{occ}}\mathrm{Tr}\psi_i^{\dagger}(\mathbf{r})\boldsymbol{\beta}\boldsymbol{\sigma}\psi_i(\mathbf{r}), \tag{2.3}$$

$$V^{\mathrm{eff}}[n(\mathbf{r}),\mathbf{m}(\mathbf{r})]=V^{\mathrm{ext}}(\mathbf{r})+\frac{\delta E_{\mathrm{xc}}[n(\mathbf{r}),\mathbf{m}(\mathbf{r})]}{\delta n(\mathbf{r})} + e^2\int\frac{n(\mathbf{r}')}{|\mathbf{r}-\mathbf{r}'|}d\mathbf{r}', \tag{2.4}$$

and

$$\mathbf{B}^{\mathrm{eff}}[n(\mathbf{r}),\mathbf{m}(\mathbf{r})]=\frac{e\hbar}{2mc}\left(\mathbf{B}^{\mathrm{ext}}(\mathbf{r})+\frac{\delta E_{\mathrm{xc}}[n(\mathbf{r}),\mathbf{m}(\mathbf{r})]}{\delta\mathbf{m}(\mathbf{r})}\right). \tag{2.5}$$

In the above equations $\boldsymbol{\alpha}$ and $\boldsymbol{\beta}$ are the standard Dirac matrices, $\boldsymbol{\sigma}$ are 4×4 Pauli spin matrices, $\mathbf{B}^{\mathrm{ext}}(\mathbf{r})$ is the external magnetic field coupling to the electron spin only, E_{xc} is the relativistic exchange-correlation energy, and ψ_i is a four-spinor. Within the local approximation, the total energy of the system can be written as

$$E[n(\mathbf{r}),\mathbf{m}(\mathbf{r})]=\int^{E_F}\varepsilon n(\varepsilon)d\varepsilon-\frac{e^2}{2}\int\int\frac{n(\mathbf{r})n(\mathbf{r}')}{|\mathbf{r}-\mathbf{r}'|}d\mathbf{r}d\mathbf{r}'-\int\left(\frac{\delta E_{\rm xc}[n(\mathbf{r}),\mathbf{m}(\mathbf{r})]}{\delta n(\mathbf{r})}n(\mathbf{r})-\frac{\delta E_{\rm xc}[n(\mathbf{r}),\mathbf{m}(\mathbf{r})]}{\delta\mathbf{m}(\mathbf{r})}\cdot\mathbf{m}(\mathbf{r})\right)d\mathbf{r}+E_{\rm xc}[n(\mathbf{r}),\mathbf{m}(\mathbf{r})],\quad(2.6)$$

where $n(\varepsilon)$ is the Kohn-Sham-Dirac single-particle density of states, and E_F is the Fermi energy of the system.

We recall the key equations of the SPR-KKR-CPA formalism in Sec. II A and in Sec. II B we derive an expression for the magnetocrystalline anisotropy energy of disordered alloys.

A. SPR-KKR-CPA formalism

The electronic Green's function for a system of relativistic spin-polarized scattering centres can be written as[37,49]

$$G(\mathbf{r},\mathbf{r}';E)=\sum_{\Lambda\Lambda'}Z^R_\Lambda(\mathbf{r};E)\tau^{00}_{\Lambda\Lambda'}(E)Z^L_{\Lambda'}(\mathbf{r}';E)-\sum_\Lambda Z^R_\Lambda(\mathbf{r}_<;E)J^L_\Lambda(\mathbf{r}_>;E),\quad(2.7)$$

where $Z^R_\Lambda(\mathbf{r};E)$ and $Z^L_\Lambda(\mathbf{r};E)$ are, respectively, the right-hand-side and left-hand-side regular solutions, and $J^L_\Lambda(\mathbf{r};E)$ is the left-hand-side irregular solution of the Kohn-Sham-Dirac equation for a single scatterer,[50] and $\tau^{00}_{\Lambda\Lambda'}(E)$ is the site-diagonal path-operator matrix. The index Λ represents the elements of various matrices according to the adopted representation. For an ordered system, $\tau^{00}_{\Lambda\Lambda'}$ can be obtained from the Brillouin zone integration

$$\tau^{00}_{\Lambda\Lambda'}(E)=\frac{1}{\Omega_{\rm BZ}}\int[t^{-1}(E)-g(\mathbf{k};E)]^{-1}_{\Lambda\Lambda'}d\mathbf{k},\quad(2.8)$$

where $g(\mathbf{k};E)$ is the KKR structure constant matrix and t is the single-site scattering matrix. For a binary disordered alloy A_xB_{1-x}, the effective t matrix is determined by the CPA condition

$$\tau^{00}_{\rm CPA}=x\tau^{00}_A+(1-x)\tau^{00}_B,\quad(2.9)$$

where

$$\tau^{00}_{A(B)}=[t^{-1}_{A(B)}-t^{-1}_{\rm CPA}+(\tau^{00}_{\rm CPA})^{-1}]^{-1}.\quad(2.10)$$

In Eqs. (2.9) and (2.10) we have suppressed the quantum number index Λ. In all subsequent discussions we will continue to do so unless it is essential to write the index. Once we have determined the Green's function we can calculate the density of states, by

$$n(E)=-\frac{1}{\pi}\Im\int{\rm Tr}G(\mathbf{r},\mathbf{r};E)d\mathbf{r}.\quad(2.11)$$

B. Magnetocrystalline anisotropy

We start from the total energy of a system within the local approximation of the relativistic spin-polarized density functional formalism, as given by Eq. (2.6). The change in the total energy of the system caused by the change in the direction of the magnetization is defined as the magnetocrystalline anisotropy energy, i.e.,

$$\Delta E=E[n(\mathbf{r}),\mathbf{m}(\mathbf{r};\mathbf{e}_1)]-E[n(\mathbf{r}),\mathbf{m}(\mathbf{r};\mathbf{e}_2)],\quad(2.12)$$

where $\mathbf{m}(\mathbf{r};\mathbf{e}_1)$ and $\mathbf{m}(\mathbf{r};\mathbf{e}_2)$ are the magnetization vectors pointing along two directions $\mathbf{e}_1$ and $\mathbf{e}_2$, respectively, the magnitudes being identical. Considering the stationarity of the energy functional and the local approximation, the contribution to ΔE is predominantly from the single-particle term in the total energy. Thus, now we have

$$\Delta E=\int^{E_{F_1}}n(\varepsilon;\mathbf{e}_1)\varepsilon d\varepsilon-\int^{E_{F_2}}n(\varepsilon;\mathbf{e}_2)\varepsilon d\varepsilon,\quad(2.13)$$

where $n(\varepsilon;\mathbf{e}_1)$ and $n(\varepsilon;\mathbf{e}_2)$ are the single-particle density of states, when the magnetic moments are pointing along $\mathbf{e}_1$ and $\mathbf{e}_2$, respectively, and E_{F_1} and E_{F_2} are the corresponding Fermi energies. We know that

$$\int^{E_F}n(\varepsilon)\varepsilon d\varepsilon=ZE_F-\int^{E_F}N(\varepsilon)d\varepsilon,\quad(2.14)$$

where Z is the total number of electrons per atom in the system and $N(\varepsilon)$ is the integrated density of states. Putting Eq. (2.14) in Eq. (2.13) and using a Taylor expansion of $N(\varepsilon;\mathbf{e}_2)$ about E_{F_2}, we obtain

$$\Delta E=-\int^{E_{F_1}}[N(\varepsilon;\mathbf{e}_1)-N(\varepsilon;\mathbf{e}_2)]d\varepsilon-\frac{1}{2}n(E_{F_2};\mathbf{e}_2)\times(E_{F_1}-E_{F_2})^2+O(E_{F_1}-E_{F_2})^3.\quad(2.15)$$

In most of the cases, the second term is expected to be very small compared to ΔE. The first term which contains the predominant contribution to ΔE needs to be evaluated accurately. Staunton *et al.*[35] and Gubanov *et al.*[53] have shown that use of Lloyd formula for the integrated density of states[54] in Eq. (2.15) leads to a more convenient expression. We use the Lloyd formula for the integrated density of states of a disordered alloy in Eq. (2.15) to get

$$\Delta E=-\frac{1}{\pi}\Im\int^{E_{F_1}}d\varepsilon\times\left[\frac{1}{\Omega_{\rm BZ}}\int d\mathbf{k}\ln\|I+[t_c^{-1}(\mathbf{e}_2)-t_c^{-1}(\mathbf{e}_1)]\tau_c(\mathbf{k};\mathbf{e}_1)\|+x\{\ln\|D_A(\mathbf{e}_1)\|-\ln\|D_A(\mathbf{e}_2)\|\}+(1-x)\{\ln\|D_B(\mathbf{e}_1)\|-\ln\|D_B(\mathbf{e}_2)\|\}\right]-\frac{1}{2}n(E_{F_2};\mathbf{e}_2)(E_{F_1}-E_{F_2})^2+O(E_{F_1}-E_{F_2})^3.\quad(2.16)$$

In Eq. (2.16), $t_c(\mathbf{e}_1)$ and $t_c(\mathbf{e}_2)$ are the SPR-KKR-CPA t matrices for magnetization along $\mathbf{e}_1$ and $\mathbf{e}_2$ directions, respectively,

$$\tau_c(\mathbf{k};\mathbf{e}_1)=[t_c^{-1}(\mathbf{e}_1)-g(\mathbf{k})]^{-1} \tag{2.17}$$

and

$$D_A(\mathbf{e}_1)=[I-\tau_c^{00}(\mathbf{e}_1)\{t_c^{-1}(\mathbf{e}_1)-t_A^{-1}(\mathbf{e}_1)\}]^{-1} \tag{2.18}$$

with similar expressions for $D_A(\mathbf{e}_2)$, $D_B(\mathbf{e}_1)$, and $D_B(\mathbf{e}_2)$. Note that $t_A(\mathbf{e}_2)$ and $t_B(\mathbf{e}_2)$ can be obtained directly from $t_A(\mathbf{e}_1)$ and $t_B(\mathbf{e}_1)$, respectively, by simple rotational transformation

$$t_{A(B)}(\mathbf{e}_2)=R(\alpha\beta\gamma)t_{A(B)}(\mathbf{e}_1)R^{\dagger}(\alpha\beta\gamma). \tag{2.19}$$

In the above equation, $R(\alpha\beta\gamma)$ is the rotation matrix corresponding to the Euler angles α, β, and γ of the direction $\mathbf{e}_2$ with respect to the direction $\mathbf{e}_1$.[51] However, for the CPA medium, this transformation will not hold as the CPA t matrix is related to the symmetry in the $\mathbf{k}$ space (through the path operator and the CPA condition) and the symmetry operations for two directions of magnetization are not same.[52] Therefore, we need to solve the SPR-KKR-CPA equations for the two magnetization directions separately to obtain $t_c(\mathbf{e}_1)$ and $t_c(\mathbf{e}_2)$.

For a pure metal, Eq. (2.16) reduces to

$$\Delta E=-\frac{1}{\pi}\Im\int^{E_{F_1}}d\varepsilon \times\left[\frac{1}{\Omega_{\mathrm{BZ}}}\int d\mathbf{k}\ln\|I+[t^{-1}(\mathbf{e}_2)-t^{-1}(\mathbf{e}_1)]\tau(\mathbf{k};\mathbf{e}_1)\|\right] -\frac{1}{2}n(E_{F_2};\mathbf{e}_2)(E_{F_1}-E_{F_2})^2+O(E_{F_1}-E_{F_2})^3 \tag{2.20}$$

and if we use the relation $\|t(\mathbf{e}_2)\|=\|t(\mathbf{e}_1)\|$ [which is true for pure metals, by virtue of Eq. (2.19)], Eq. (2.20) reduces to the expression given by Staunton *et al.*[35]

Note that, in Eqs. (2.16) and (2.20), the upper limit of energy integration is E_{F_1}, the Fermi energy of the system when the magnetization is along $\mathbf{e}_1$. The contribution to ΔE due to the difference in the two Fermi levels is of the order of $(E_{F_1}-E_{F_2})^2$. This contribution is expected to be very small, but nevertheless, it can be approximately estimated as follows. We have

$$N(E_{F_1};\mathbf{e}_2)=Z+\Delta Z, \tag{2.21}$$

where ΔZ is the deviation in the total number of electrons (Z) due to incorrect Fermi energy for the magnetization along $\mathbf{e}_2$. Since $Z=N(E_{F_1};\mathbf{e}_1)$, ΔZ is the difference in the integrated density of states for the two magnetization directions at the energy E_{F_1}. Thus, with the help of Lloyd's formula, we can write

$$\Delta Z=\frac{1}{\pi}\Im\left[\frac{1}{\Omega_{\mathrm{BZ}}}\int d\mathbf{k}\ln\|\{I+[t_c^{-1}(E_{F_1};\mathbf{e}_2) -t_c^{-1}(E_{F_1};\mathbf{e}_1)]\tau_c(\mathbf{k},E_{F_1};\mathbf{e}_1)\}\|+x\{\ln\|D_A(E_{F_1};\mathbf{e}_1)\| -\ln\|D_A(E_{F_1};\mathbf{e}_2)\|\}+(1-x)\{\ln\|D_B(E_{F_1};\mathbf{e}_1)\| -\ln\|D_B(E_{F_1};\mathbf{e}_2)\|\}\right]. \tag{2.22}$$

We can then use this value of ΔZ to determine E_{F_2} from Eq. (2.21) by rewriting it as

$$\Delta Z=\int_{E_{F_2}}^{E_{F_1}}n(\varepsilon;\mathbf{e}_2)d\varepsilon. \tag{2.23}$$

In real applications, E_{F_1} and E_{F_2} are expected to be very close. Therefore, we can approximate Eq. (2.23) using the trapezoidal rule as

$$\Delta Z\approx\frac{1}{2}(E_{F_1}-E_{F_2})[n(E_{F_1};\mathbf{e}_2)+n(E_{F_2};\mathbf{e}_2)]. \tag{2.24}$$

Thus we have

$$\frac{1}{2}n(E_{F_2};\mathbf{e}_2)(E_{F_1}-E_{F_2})^2\approx\frac{2(\Delta Z)^2n(E_{F_2};\mathbf{e}_2)}{[n(E_{F_1};\mathbf{e}_2)+n(E_{F_2};\mathbf{e}_2)]^2}. \tag{2.25}$$

In most of the metals and their alloys, $n(E_{F_1};\mathbf{e}_2)$ and $n(E_{F_2};\mathbf{e}_2)$ are at least of the order of 1 states/eV. Therefore, for the above term to give meaningful contribution to ΔE, we would need ΔZ to be at least of the order of 10^{-4}. Thus when ΔZ is less than 10^{-4} we can quite justifiably neglect the terms containing $(E_{F_1}-E_{F_2})^2$. In other words, in such cases, we do not need to estimate E_{F_2}; only a knowledge of E_{F_1} will suffice. Only in rare instances, should the second order term be significant.

III. COMPUTATIONAL ASPECTS

In this section we discuss computational details and practical difficulties in the calculation of MAE of disordered alloys. A good review of technical aspects of solving the Kohn-Sham-Dirac equations and calculating the KKR Green's function at real as well as complex energies is given by Strange *et al.*,[36,37] and those will not be repeated here.

We need to evaluate the energy integral as well as the Brillouin zone integral in Eq. (2.16) to a very high degree of accuracy. Therefore, it is advisable to distort the energy integration into the complex plane. In the complex plane, the integrand becomes a smooth function of energy and $\mathbf{k}$ and we need fewer energy points as well as fewer $\mathbf{k}$ points to obtain an accurate integral.[55] In our calculation, we have used a rectangular box contour starting from below the bottom of the valence band on the real axis and ending at the Fermi energy on the real axis. The top of the box contour is 1.0 Ry above the real axis where the integrand is almost featureless, and therefore, we need a very few energy points along this line. Along the two legs of the contour, in particular, nearer to the real axis we need a finer mesh. Accordingly, we have used a logarithmic mesh along the two legs of the contour. Again, if our contour starts from below the valence band, as is the case, the integrand is structureless along the

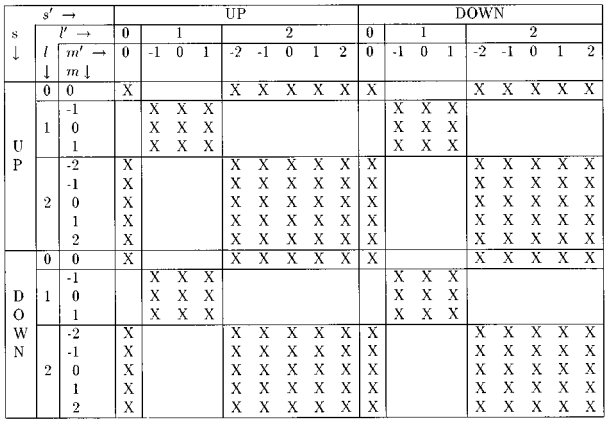

FIG. 1. The matrix structure of τ^{00} in the (lms) representation for a cubic crystal when the magnetization is along a general direction. The nonzero elements are indicated by X. The symmetry of the matrix is given by Eq. (3.1).

bottom leg as well. Thus, practically, we need a dense mesh only in the top leg of the contour. In our calculations, the number of energy points is approximately 70 (10 each in the bottom leg and on the top horizontal line, and 40–50 points in the top leg). We have checked that this number is sufficient enough to give accurate energy integrals.

The second important point is the Brillouin zone integration. Depending upon the direction of magnetization, the number of symmetry operations in the Brillouin zone will be different.[52] In a cubic crystal, the effective symmetry is tetragonal, trigonal or orthorhombic depending on whether the magnetization is along the [001], [111], or [110] directions, respectively. Because of that, the irreducible part of the Brillouin zone will be different when the direction of magnetization is altered. Strange *et al.*[37] have discussed the evaluation of the path operator for different magnetization directions. They have pointed out that, owing to the reduced symmetry in the Brillouin zone, it is necessary to perform the Brillouin zone integration in $\frac{1}{16}$th of the zone when the magnetization is along [001] direction and in $\frac{1}{4}$th of the zone when it is along a general direction (as opposed to $\frac{1}{48}$th in the nonrelativistic case). They have also shown the structure and symmetry of the path operator matrix in presence of a field along the [001] direction, in $(\kappa\mu)$ as well as (lms) representation. We refer the reader to that reference for details. In our calculation, we work throughout in the (lms) representation for the simple reason that it is more comprehensible, and moreover, there is no real advantage in working with the $(\kappa\mu)$ representation when the magnetization is along a general direction, because then all the degeneracies in the matrix elements of the path-operator are lifted. In Fig. 1, we show the structure of the path operator matrix in the (lms) representation (for $l \leqslant 2$) when the magnetization is along a general direction. We note that there are altogether 180 nonzero elements (indicated as X). The symmetry of the matrix is given by

$$\tau^{00}_{l'm's';lms} = (i)^{m-m'+s-s'} \tau^{00}_{lms;l'm's'}, \tag{3.1}$$

and therefore, there are only 99 independent elements which need to be calculated. The SPR-KKR-CPA t matrix will also have a similar structure.

For the Brillouin zone integration we have used the prism method described in detail by Stocks *et al.*[56] While solving the SPR-KKR-CPA equations, we have used 55 directions in each of the forty-eighths of the Brillouin zone. The number of **k** points per direction varies depending upon the value of imaginary part of the complex energy. Near the real axis, we have used about 200 **k** points per direction and far fewer **k** points as we go away from the real axis. Evidently, we need more **k** points for the calculation of MAE. We will discuss this later. The SPR-KKR-CPA equations were solved using the algorithm of Mills *et al.*[57] which has been proved to lead to fast convergence in earlier works.[42,58] We have obtained a self-consistency of the order of 10^{-9} in the t matrices for both magnetization directions.

In our studies, we have used the potentials generated by the self-consistent spin-polarized scalar relativistic KKR-CPA method, which gives spin-up and spin-down potentials $V_{\uparrow}(\mathbf{r})$ and $V_{\downarrow}(\mathbf{r})$. The potential and field, which we need in the fully relativistic treatment, are given by

$$V^{\text{eff}}(\mathbf{r}) = \frac{1}{2}[V_{\uparrow}(\mathbf{r}) + V_{\downarrow}(\mathbf{r})] \tag{3.2}$$

and

$$B^{\text{eff}}(\mathbf{r}) = \frac{1}{2}[V_{\uparrow}(\mathbf{r}) - V_{\downarrow}(\mathbf{r})]. \tag{3.3}$$

In previous calculations,[15,30] it was observed that MAE is quite sensitive to small inaccuracies in the Fermi energy (or equivalently, to electron filling). From Eq. (2.16) it is quite evident that, even an inaccuracy of the order of 1 mRy in the Fermi energies will affect the MAE drastically, and hence we have to determine the Fermi energy to a corresponding accuracy. As explained in the previous section, we need to calculate the Fermi energy for only one magnetization direction, namely, [001], and we can estimate the second term in Eq. (2.16) according to Eq. (2.25).

IV. RESULTS AND DISCUSSION

A. Pure elements

Before attempting a full-fledged calculation of the MAE for disordered alloys, it is worthwhile to test our theory by performing calculations for elemental solids and comparing our results with available experimental data as well as results of previous theoretical calculations. For this exercise, we have chosen bcc-Fe, fcc-Co, and fcc-Ni for which experimental as well as theoretical data exist in the literature. We found that the Fermi energy for the [001] direction of magnetization, calculated within the SPR-KKR-CPA is about 1–2 mRy above the scalar relativistic value for all the three elements. We also estimated the order of magnitude of the second term in Eq. (2.16) for these three elements, and found that, it is of the order of 10^{-2} μeV, which is one order of magnitude smaller than the first term.

In Table I, we compare our results for bcc-Fe, fcc-Co, and fcc-Ni with the experimental results as well as the results of

TABLE I. Experimental and calculated magnetocrystalline anisotropy energy, defined as $\Delta E = E(001) - E(111)$ per atom for Fe, Ni, and Co, in units of μeV. Column A is from Ref. 15, column B is from Ref. 30, column C is from Ref. 62, column D is from Ref. 28 without orbital polarization, column E is also from Ref. 28 but with orbital polarization, and column F is the present work.

Solid	Experiment	Theory					
		A	B	C	D	E	F
bcc Fe	-1.4[a]	-0.5	-9.6	7.4	-0.5	-1.8	-0.95
fcc Co	1.8[b]				0.5	2.2	0.86
fcc Ni	2.7[c]	-0.5	10.5	10.0	-0.5	-0.5	0.11

[a]Ref. 59.
[b]Ref. 60.
[c]Ref. 59,61.

previous calculations. Among the results of previous calculations, the results of Trygg *et al.*[28] (columns D and E) are closest to the experiment, and therefore, we will compare our results to theirs. Their results for bcc-Fe and fcc-Co are in good agreement with the experiment if orbital polarization is included in the calculation of MAE. However, in case of fcc-Ni, their prediction of the magnitude of MAE as well as the magnetic easy axis is not in accordance with the experiment, and even the inclusion of orbital polarization fails to improve the result. Our results for bcc-Fe and fcc-Co are also in good agreement with the experiment, predicting the correct easy axis, although the magnitude of MAE is somewhat smaller than the experimental value. Considering that in our calculations orbital polarization is not included we feel that our results are quite satisfactory. In the case of fcc-Ni, we obtain the correct easy axis of magnetization, but the magnitude of MAE is far too small compared to the experimental value. As noted earlier, in the calculation of MAE, the convergence with regards to the Brillouin zone integration is very important. We have checked this aspect and are satisfied that our results are well converged with respect to the Brillouin zone integration. In our calculation, we have used 210 directions in the irreducible wedge of the Brillouin zone and we have taken around 600 points per direction, when the energy is near the real axis, and less and less number of points as we go further to the complex plane. Compared to this, Daalderop *et al.*[15] used $\sim 500\,000$ **k** points in the irreducible part of the Brillouin zone, and Trygg *et al.*[28] used 2000 **k** points for bcc-Fe and 6000 **k** points for fcc-Co and fcc-Ni in the irreducible part of the Brillouin zone. Therefore, it seems that our method is capable of calculating the magnetocrystalline anisotropy of solids in reasonable computational time.

B. Co_xPt_{1-x} alloys

Now we present the results of our calculation of MAE for disordered fcc-Co_xPt_{1-x} alloys. We have used the atomic sphere potentials generated by the self-consistent spin-polarized scalar relativistic KKR-CPA method and constructed the spin-averaged and spin-dependent potentials according to Eqs. (3.2) and (3.3). However, we recalculated the Fermi energy by SPR-KKR-CPA method for magnetization along the [001] direction (denoted as E_{F_1}). This exercise was necessary because in previous studies on elemental solids MAE was found to be quite sensitive to the position of the Fermi level.[15,30] We found that, for all the three compositions of the alloy, the difference in the Fermi energies of the scalar relativistic and fully relativistic cases is of the order of 5 mRy which is quite large compared to the magnitude of MAE. Secondly, on rotating the magnetization direction there is a redistribution of the occupied energy bands in the Brillouin zone. This will lead to a shift in the Fermi level (denoted as E_{F_2}). The effect of this small shift in the Fermi energy on the MAE is given by the second term in Eq. (2.16) which is of the order of $(E_{F_1} - E_{F_2})^2$. This term can be calculated in terms of the difference in number of electrons between the two directions at a common Fermi energy, as given by Eq. (2.25). We calculated ΔZ using Eq. (2.22), and the values are 9.6×10^{-6}, 1.4×10^{-4}, and 2.8×10^{-5} electrons for $x = 0.25$, 0.50, and 0.75, respectively. Thus the second term of Eq. (2.16) comes out to be very small; in fact it is less than 0.01 μeV for all the three compositions. Hence, the first term of Eq. (2.16) is the dominant term and needs to be evaluated accurately.

Another important question in the calculation of MAE is the convergence of integral in Eq. (2.16) with respect to the number of **k** points used in the Brillouin zone. We have calculated the MAE of Co_xPt_{1-x} alloys as a function of number of **k** points in the irreducible wedge of the Brillouin zone. In our calculations, as stated earlier, we have used a complex energy contour for energy integration. We use fewer points when we are far removed from the real axis, and gradually increase the number of points as we come closer to the real axis. In Fig. 2 we plot the MAE as a function of number of **k** points (in the irreducible wedge of the Brillouin zone) for the energy on the real axis. We note that quite a large number of **k** points is needed to get a convergence. Thus if we do not use an appropriate contour in the complex energy plane, we would have to use this many points for each energy requiring an enormous computational effort. This underlines the importance of using the complex energy plane in such calculations. Moreover, we also study the MAE as a function of temperature by using Fermi-Dirac distribution in the energy integration. The energy integrals are then transformed into sums over the poles of the Fermi factor.[63]

In Fig. 3 we show the MAE of disordered fcc-Co_xPt_{1-x} alloys for $x = 0.25$, 0.5, and 0.75 as a function of temperature between 0 and 1500 K. We note that for all the three compositions, MAE is positive at all temperatures implying that

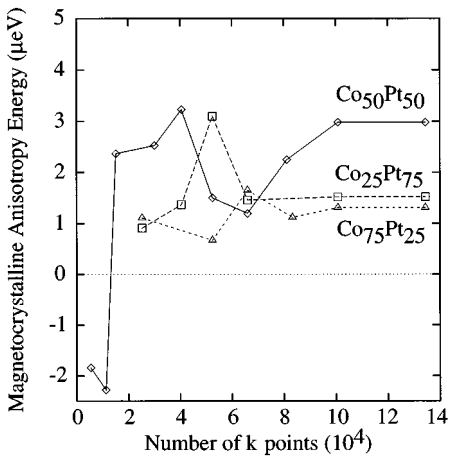

FIG. 2. Convergence of the magneto6rystalline anisotropy energy of Co_xPt_{1-x} alloys for $x=0.25$, 0.50, and 0.75, as a function of number of **k** points in the irreducible wedge of the Brillouin zone.

the magnetic easy axis is always along the [111] direction of the crystal, though the magnitude of MAE decreases with the increase in the temperature. We recall that the magnetic easy axis of fcc-Co is also along the [111] direction but the magnitude of MAE is smaller. Thus, alloying with Pt does not alter the magnetic easy axis. We also note that the equiatomic composition has the largest MAE which is about 3.0 μeV at 0 K. In these alloys, one component (Co) has strong magnetic moment but weak spin-orbit coupling, while in the other component (Pt) spin-orbit coupling is strong but the magnetic moment is small. Addition of Pt to Co results in a monotonic decrease in the average magnetic moment of the system[38,39] but the spin-orbit coupling becomes stronger. Around the equiatomic composition, both the magnetic moment as well as the spin-orbit coupling are significant, for other compositions either the magnetic moment or the spin-orbit coupling is weaker. We expect that this is the reason for MAE being largest for the equiatomic composition.

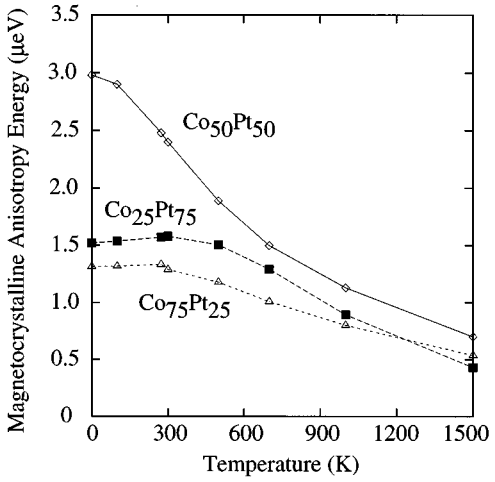

FIG. 3. Magnetocrystalline anisotropy energy of Co_xPt_{1-x} alloys for $x=0.25$, 0.50, and 0.75, as a function of temperature.

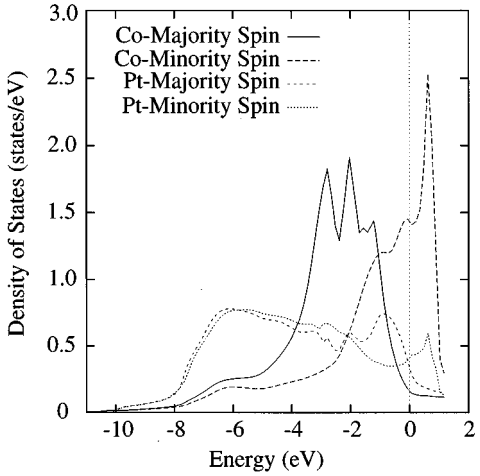

FIG. 4. Spin-resolved density of states for Co and Pt in fcc-$Co_{0.5}Pt_{0.5}$ alloy for magnetization along the [001] direction of the crystal. The vertical dotted line indicates the Fermi level. The calculations have been done with an imaginary part of 1.4×10^{-4} eV in the energy.

We can understand the magnetocrystalline anisotropy of a system in terms of its electronic structure. In Fig. 4 we show the spin-resolved density of states on Co and Pt atoms in $Co_{0.50}Pt_{0.50}$ alloy for magnetization along the [001] direction. We observe that Pt density of states is rather structureless except around the Fermi energy where there is spin splitting due to hybridization with Co *d* bands. When the direction of magnetization is altered to [111] direction of the crystal the electronic structure also changes due to redistribution of the electrons, but the difference is quite small and difficult to visualize. Therefore, in Fig. 5 we have plotted the difference in the density of states for the two directions of magnetization. We note that, in the lower part of the band

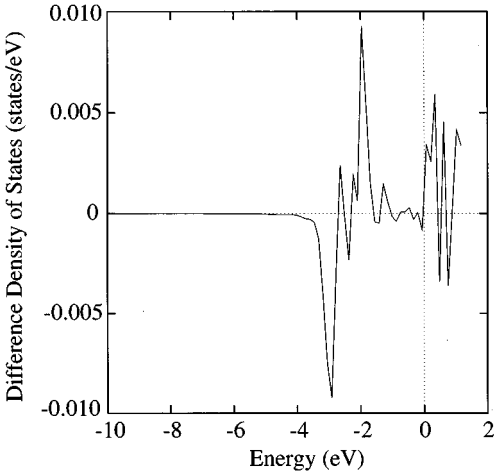

FIG. 5. The difference between the densities of states of fcc-$Co_{0.5}Pt_{0.5}$ alloy for magnetization along the [001] and [111] directions of the crystal. The vertical dotted line indicates the Fermi level. The separation between two Fermi levels is less than the thickness of this line.

which is Pt dominated, there is little difference between the two. And it is quite oscillatory in the upper part dominated by Co *d*-band complex. We also observe spikes at energies where there are peaks in the Co density of states. Due to the oscillatory nature of this curve, the magnitude of MAE is quite small; the two large peaks around 2 and 3 eV below the Fermi energy almost cancel each other and only the smaller peaks contributing to the MAE. Also, due to this oscillatory behavior, a shift in the Fermi level will alter the magnitude as well as the sign of the MAE. This was also observed in previous studies on elemental solids.[15,30] This curve also tells us that states far removed from the Fermi level (in this case, 4 eV below the Fermi level) can also contribute to the MAE, and not just the electrons on the Fermi surface.

In contrast to what we have found for the disordered fcc phase of Co_xPt_{1-x} alloys, in the ordered tetragonal CoPt alloy MAE is quite large (~ 400 μeV) and, more importantly, the magnetic easy axis is along the *c* axis.[6] Theoretical calculations of MAE for the ordered tetragonal CoPt alloy[21,22] based on scalar relativistic methods do reproduce the correct easy axis but overestimate the MAE by a factor of 2. At this stage it is not clear, whether it is the atomic ordering or the loss of cubic symmetry of the crystal in the tetragonal phase, which is responsible for altogether different magnetocrystalline anisotropies in disordered and ordered CoPt alloys. However, we believe that it is a combined effect of the two and intend to study the effect of atomic short-range order on the magnetocrystalline anisotropy of alloys as the next step. In our calculations, we have assumed that the orbital angular momentum is quenched, and so the inclusion of orbital polarization in the calculation may also affect these results. In principle, orbital polarization can be included in the theory by using current-density functional theory.[64] We are now working along these lines.

V. CONCLUSIONS

We presented a first-principles method to calculate the magnetocrystalline anisotropy of disordered alloys based on the SPR-KKR-CPA scheme. In our theory, relativistic effects such as the spin-orbit coupling and spin-polarization are treated on an equal footing. Before attempting a study of the MAE for complex systems such as disordered alloys, we felt it necessary to assess our method by using it to study the MAE of systems for which experimental as well as previous theoretical results exist in the literature. We have done this by calculating the MAE of bcc-Fe, fcc-Co, and fcc-Ni. We found good agreement with the experimental as well as previous theoretical results. Then we calculated the MAE of disordered fcc-Co_xPt_{1-x} alloys for $x=0.25$, 0.5, and 0.75. We found that, for all the three compositions, the magnetic easy axis is along the [111] direction of the crystal and anisotropy is largest for $x=0.50$. We also found that states far removed from the Fermi level can also contribute to the MAE, and that, a slight shift in the Fermi level might alter the magnitude of MAE as well as the direction of the magnetic easy axis. Thus, the Fermi level needs to be evaluated very accurately. The other factor in the calculation of MAE is the Brillouin zone integration which must be performed with great care. We also pointed out that there is a need to include the effects of atomic short-range order, orbital polarization, etc., in the calculation of MAE of alloys.

ACKNOWLEDGMENTS

This research is supported by the Engineering and Physical Sciences Research Council (UK) and National Science Foundation (USA).

[1] L. M. Falicov, D. T. Pierce, S. D. Bader, R. Gronsky, K. H. Hathaway, H. J. Hopster, D. N. Lambeth, S. P. Parkin, G. Prinz, M. Salamon, I. K. Schuller, and R. H. Victora, J. Mater. Res. **5**, 1299 (1990).

[2] S. D. Bader, Proc. IEEE **78**, 909 (1990).

[3] T. Wakiyama, in *Physics and Engineering Applications of Magnetism*, edited by Y. Ishikawa and N. Miura (Springer-Verlag, Berlin, 1991), p. 133.

[4] J. Stör and H. König, Phys. Rev. Lett. **75**, 3748 (1995), and references therein.

[5] D. Weller, J. Stöhr, R. Nakajima, A. Carl, M. G. Samant, C. Chappert, R. Megy, P. Beauvillain, P. Veillet, and G. A. Held, Phys. Rev. Lett. **75**, 3752 (1995), and references therein.

[6] G. Hadjipanayis and P. Gaunt, J. Appl. Phys. **50**, 2358 (1979).

[7] C. J. Lin and G. L. Gorman, Appl. Phys. Lett. **61**, 1600 (1992).

[8] D. Weller, H. Brandle, C. J. Lin, and H. Notary, Appl. Phys. Lett. **61**, 2726 (1992).

[9] D. Weller, H. Brandle, and C. Chappert, J. Magn. Magn. Mater. **121**, 461 (1993).

[10] D. Weller, G. R. Harp, R. F. C. Farrow, A. Cebollada, and J. Sticht, Phys. Rev. Lett. **72**, 2097 (1994).

[11] T. Suzuki, D. Weller, C. A. Chang, R. Savoy, T. C. Huang, B. Gurney, and V. Speriosu, Appl. Phys. Lett. **64**, 2736 (1994).

[12] M. Maret, M. C. Cadeville, W. Staiger, E. Beaurepaire, R. Poinsot, and A. Herr, Thin Solid Films **275**, 224 (1996).

[13] T. A. Tyson, S. D. Conradson, R. F. C. Farrow, and B. A. Jones, Phys. Rev. B **54**, R3702 (1996).

[14] J. G. Gay and R. Richter, Phys. Rev. Lett. **56**, 2728 (1986).

[15] G. H. O. Daalderop, P. J. Kelly, and M. F. H. Schuurmans, Phys. Rev. B **41**, 11 919 (1990).

[16] G. Y. Guo, W. M. Temmerman, and H. Ebert, J. Phys.: Condens. Matter **3**, 8205 (1991).

[17] G. Y. Guo, W. M. Temmerman, and H. Ebert, Physica B **172**, 61 (1991).

[18] G. H. O. Daalderop, P. J. Kelly, and F. J. A. den Broeder, Phys. Rev. Lett. **68**, 682 (1992).

[19] R. H. Victora and J. M. MacLaren, Phys. Rev. B **47**, 11 583 (1993).

[20] M. Cinal, D. M. Edwards, and J. Mathon, Phys. Rev. B **50**, 3754 (1994).

[21] A. Sakuma, J. Phys. Soc. Jpn. **63**, 3053 (1994).

[22] I. V. Solovyev, P. H. Dederichs and I. Mertig, Phys. Rev. B **52**, 13 419 (1995), and references therein.

[23] D. S. Wang, R. Wu, and A. J. Freeman, Phys. Rev. Lett. **70**, 869 (1993).

[24] G. H. O. Daalderop, P. J. Kelly, and M. F. H. Schuurmans, Phys. Rev. Lett. **71**, 2165 (1993).

[25] D. S. Wang, R. Wu, and A. J. Freeman, Phys. Rev. Lett. **71**, 2166 (1993).
[26] X. D. Wang, R. Wu, D. S. Wang, and A. J. Freeman, Phys. Rev. B **54**, 61 (1996); X. D. Wang, A. J. Freeman, R. Wu, and D. S. Wang, J. Appl. Phys. **79**, 5827 (1996).
[27] R. Wu and A. J. Freeman, J. Appl. Phys. **79**, 6209 (1996), and references therein.
[28] J. Trygg, B. Johansson, O. Eriksson, and J. M. Wills, Phys. Rev. Lett. **75**, 2871 (1995).
[29] P. Strange, H. Ebert, J. B. Staunton, and B. L. Gyorffy, J. Phys.: Condens. Matter **1**, 3947 (1989).
[30] P. Strange, J. B. Staunton, B. L. Gyorffy, and H. Ebert, Physica B **172**, 51 (1991).
[31] P. Strange, J. B. Staunton, and H. Ebert, Europhys. Lett. **9**, 169 (1989).
[32] H. Brooks, Phys. Rev. **58**, B909 (1940).
[33] A. R. Mackintosh and O. K. Andersen, in *Electrons at the Fermi Surface*, edited by M. Springfold (Cambridge University Press, Cambridge, 1980); M. Weinert, R. E. Watson, and J. W. Davenport, Phys. Rev. B **32**, 2115 (1985).
[34] H. J. F. Jansen, Phys. Rev. B **38**, 8022 (1988).
[35] J. B. Staunton, M. Matsumoto, and P. Strange, in *Applications of Multiple Scattering Theory to Materials Science*, edited by W. H. Butler, P. H. Dederichs, A. Gonis, and R. L. Weaver, MRS Symposia Proceedings No. 253 (Materials Research Society, Pittsburgh, 1992), p. 309.
[36] P. Strange, J. B. Staunton, and B. L. Gyorffy, J. Phys. C **17**, 3355 (1984).
[37] P. Strange, H. Ebert, J. B. Staunton, and B. L. Gyorffy, J. Phys.: Condens. Matter **1**, 2959 (1989).
[38] H. Ebert and H. Akai, in *Applications of Multiple Scattering Theory to Materials Science* (Ref. 35), p. 329.
[39] H. Ebert, B. Drittler, and H. Akai, J. Magn. Magn. Mater. **104-107**, 733 (1992).
[40] H. Ebert and H. Akai, in *Physics of Transition Metals*, edited by P. M. Oppeneer and J. Kübler (World Scientific, Singapore, 1992), p. 922.
[41] H. Ebert, H. Akai, H. Maruyama, A. Koizumi, H. Yamazaki, and G. Shutz, in *Physics of Transition Metals* (Ref. 40), p. 750.
[42] H. J. Gotsis, P. Strange, and J. B. Staunton, Solid State Commun. **92**, 449 (1994).
[43] G. Y. Guo, W. M. Temmerman, P. J. Durhand, and H. Ebert, J. Magn. Magn. Mater. **148**, 66 (1995).
[44] H. Ebert, G. Y. Guo, and G. Schütz, IEEE Trans. Magn. **31**, 3301 (1995).
[45] For a recent review see, e.g., H. Ebert, Rep. Prog. Phys. **59**, 1665 (1996).
[46] A. H. MacDonald and S. Vosko, J. Phys. C **12**, 2977 (1979).
[47] A. K. Rajagopal, J. Phys. C **11**, L943 (1978).
[48] M. V. Ramana and A. K. Rajagopal, Adv. Chem. Phys. **54**, 231 (1983).
[49] J. S. Faulkner and G. M. Stocks, Phys. Rev. B **21**, 3222 (1980).
[50] E. Tamura, Phys. Rev. B **45**, 3271 (1992).
[51] A. Messiah, *Quantum Mechanics* (North-Holland, Amsterdam, 1965), Vol. 2.
[52] A. P. Cracknell, J. Phys. C **2**, 1425 (1969).
[53] V. A. Gubanov, A. I. Liechtenstein, and A. V. Postnikov, *Magnetism and the Electronic Structure of Crystals*, Vol. 98 of Springer Series in Solid State Sciences (Springer-Verlag, Berlin, 1992).
[54] P. Lloyd, Proc. Phys. Soc. London **90**, 207 (1967).
[55] R. Zeller, J. Deutz, and P. H. Dederichs, Solid State Commun. **44**, 993 (1982).
[56] G. M. Stocks, W. M. Temmerman, and H. Winter, in *Electrons in Disordered Metals and at Metallic Surfaces*, Vol. 42 of NATO Advanced Study Institute Series B: Physics, edited by P. Phariseau, B. L. Gyorffy, and L. Scheire (Plenum, New York, 1979).
[57] R. Mills, L. J. Gray, and T. Kaplan, Phys. Rev. B **27**, 3252 (1983).
[58] B. Ginatempo and J. B. Staunton, J. Phys. F **18**, 1827 (1988).
[59] C. J. Tung, I. Said, and G. E. Everett, J. Appl. Phys. **53**, 2044 (1982).
[60] T. Suzuki, as quoted in Ref. 28.
[61] R. Gersdorf, Phys. Rev. Lett. **40**, 344 (1978).
[62] H. Eckardt, L. Fritsche, and J. Noffke, J. Phys. F **17**, 943 (1987).
[63] K. Wildberger, P. Lang, R. Zeller, and P. H. Dederichs, Phys. Rev. B **52**, 11 502 (1995).
[64] H. Ebert and M. Battocletti, Solid State Commun. **98**, 785 (1996); H. Ebert, M. Battocletti, and E.K.U. Gross (unpublished).